Original Article

Recent Research in Science and Technology 2016, 8: 6-13
http://scienceflora.org/journals/index.php/rrst/
doi: 10.19071/rrst.2016.v8.2914

Influence of H^+ ion on microstructure and electrochemical behavior passive film formed on stainless steel-304 in low concentrated sulfuric acids

R. Natarajan*

Department of Chemistry, Alagappa Government Arts College, Karaikudi, Sivaganga, Tamil Nadu, India

Received: 11.12.2015
Accepted: 22.03.2016
Published: 13.04.2016

***Address for correspondence:**
R. Natarajan, Department of Chemistry, Alagappa Government Arts College, Karaikudi, Sivaganga, Tamil Nadu, India.
Email: nataraajan12@yahoo.co.in

ABSTRACT

The investigation focused toward microstructure and electrochemical changes caused by proton on a passive film formed on the surface of stainless steel-304 in lower concentrated sulfuric acid solutions (exclusively 0.5, 1.0, 2.0, and 5.0 N concentrations). Dissociation rate of the proton in the acid was reduced due to increasing of acid concentration from 0.5 to 5.0 N, which causes anodic shift at open circuit potential region and cathodic shift in different passivation potential regions. Proton enhances different electrochemical behaviors such as activation, primary, secondary passive, and transpassive behaviors, which was concluded by increasing of current value in these regions. AC impedance parameters such as double layer capacitance (C_{dl}), charge transfer resistance (R_{ct}) are compared with selective polarization parameters. Microstructure and chemical entities present in the passive film were examined through scanning electron microscopy and X-ray photoelectron spectroscopic techniques. The role of H^+ and SO_4^{2-} ion on metal dissolution and passive film formation have been discussed.

KEY WORDS: Acid solutions, passivity, potentiodynamic polarization, stainless steel

INTRODUCTION

The Large scale of sulfuric acid manufacturing is done in throughout the world since it not only employed as a vital source for inorganic acids such as HNO_3 and H_3PO_4 preparation but also in plant manure, readymade food articles, medicine, coloring materials used in textile and paper industries, and other chemical production process. In higher concentration (70-95%), the severity of corrosiveness is negligible. During the period of preparation, freight and hauling, much consideration needs to be in diluted conditions. There it produces aggressive corrosive environment and cause severe damage to handling materials. Manufacture of sulfuric acid from SO_3 results heat emission and pressure development inside of the container. In higher concentrations, its severity of aggressiveness is negligible, where carbon steel materials was carbon steel materials can be used, but in diluted conditions, stainless steels are exclusive candidate materials for handling sulfuric acid, the impurities present in the acid also enhances corrosion problem. The active-passive nature of stainless steels results dissolution of its chemical constituents reduced the quality of acids and produce unwanted additional products (Riggs and Locke, 1981). As an anti-scaling agent sulfuric acid results deleterious effect (Jamialahmadi and Muller-Steinhagen, 2007; Louie, 2008). Conventional austenitic stainless steels posses corrosion resistance in very dilute or higher concentrated acids and slightly elevated temperature (ASM, 2005).

The corrosion problem and its mechanism of SS-304 in some lower concentrated (0.1, 0.3, 0.5, 0.7, 0.9, and 1.0 M) sulfuric acid are investigated (Abdallah, 2003). Electrochemical protection technique such as passivation method is used to prevent for mineral acid corrosion observed in storage tank. In diluted condition, the H^+ ion and its counter ion present in the sulfuric acid activate dissolution of stainless steel (Hermas and Morad, 2008). A number of workers registered their observation in literature (Kish *et al*., 2003; Raja and Jones, 2006; Ren and Zeng, 2007; and Kumagai *et al*., 2008) for passivation property of stainless steel-304 in sulfuric acid. The goal of our present work is to concentrate the active-passive mechanism of SS-304 in certain diluted concentrations at various anodic polarized potential points. The microstructure and chemical entities present in the passive

layer are analyzed through scanning electron microscope (SEM) and electron spectroscopy for chemical analyzer (ESCA) techniques. It will be hope that this present work will fulfill and provide some improved information in the understanding of reaction mechanism observed in some lower critical normality ranges of H_2SO_4 used in the industrial application.

EXPERIMENT

Materials

The individual elements present in the stainless steel-304 are presented in Table 1. The rod- shaped steel sample received from commercial supplier having 1 cm dia. For potentiodynamic polarization and AC impedance studies, working electrode having 0.5 cm diameter was used. Other surface area was masked using Teflon material. The smooth surface of the electrode was prepared using silicon carbide emery papers 1/0 to 4/0 to mirror finishing, followed by degreased with acetone, and finally rinsed with triple distilled water. For SEM and ESCA studies, the specimens having 1 cm^2 surface area were used. Sulfuric acid used as electrolyte in the diluted form having analytical reagent grade with assay 99%, and the density is 1.835 g/cc. The acid diluted by triple distilled water to required concentration. The electrolyte used for the study was in atmospheric exposed condition.

Methods

A three electrode cell assembly consisting stainless steel, 2 cm^2 area of Pt mesh and saturated calomel electrode are employed as a working, counter, and reference electrodes, respectively. To avoiding electrolytic contamination, the reference electrode was connected through a salt bridge. The scan rate of anodic polarization study was 1 mV/s; the iR compensation was done for 15 min. Polarization diagram was recorded using potential (V) versus log current (i), EG&G Princeton Applied Research (PAR) model 173 Potentiostat with EG&G PAR model 175 programmer connected to Rikadenki X-Y recorder were used to carried out the polarization study at the scanning potential range from −450 to 800 mV. EG&G PAR model 6310 electrochemical impedance system was used for impedance measurements. Amplitude of 10 mV is used for AC signal to all EIS measurements. From the Bode plots (Frequency (Hz) vs. log |Z|) the impedance parameters such as charge transfer resistance (R_{ct}) and solution resistance (R_s) were calculated. The scanning frequency range is from 0.100 to 10,000 Hz. All the experiments were repeated thrice for reproducibility. The double layer capacitance value (C_{dl}) is calculated from the following equation.

$$C_{dl} = 1/2\pi f_{max} \times R_{ct} \quad (1)$$

From Nyquist plot the maximum frequency (f_{max}) is obtained. The film formed on the surface of the electrode is to be kept constantly for 1 h at respective passive potential regions in 0.5 N acid environment. SEM (Hitachi- Keeping model S-3000H) was used to view the microstructure of surface.

VG scientific mark II ESCA Spectrometer was used for examine the chemical entities present in the passive film formed on the surface. The specimen was kept for about an hour in the potentials points of C and E in 0.5 N and 5.0 N H_2SO_4 solutions to enable to form passive layer on the surface. The surface was dried and examined. To investigate the nature and valancies of the constituent elements of passive film formed, the specimen was analyzed using X-ray photoelectron spectroscopy (XPS) Mg Kα having mean energy of 1253.6 eV was used for irradiation. The voltage and current applied in the X-ray tube were 8 kV and 100 Ma, respectively. The specimen container was evacuated to 10^{-9} m bar.

Hydrocarbon contamination having C_{1s} binding energy and 285 eV was used as calibration to compensate the charging system. An adsorbed contaminants deposited on the surfaces was removed using delocalized Ar+ ion beam accelerated under 2 KeV. Fe2p, Cr2p, Ni2p, Mn2p, S2p, and O2p electron levels are used to measure for record the photoelectron spectra.

Table 1: Chemical entity present in the stainless steel-304 in weight percentage

Elements	Cr	Ni	Mn	C	Si	P	S	Iron
Percentage	18.29	8.75	1.86	0.87	0.065	0.039	0.026	Rest

EXPERIMENTAL RESULTS

Potentiodynamic Polarization Study

Figure 1 shows anodic polarization curves obtained from stainless steel-304 exposed in sulfuric acid solution having 0.5, 1.0, 2.0, and 5.0 N concentrations.

Table 2 shows the Tafel polarization parameters obtained from the curves. Open circuit potentials (OCP) for stainless steel-304 in different concentrations of H_2SO_4 solution are in between −450 and −380 mV. The polarization started at −450 mV for all concentration of acid are pointed out. Metallic dissolution and passive film formation process were obtained at two potential points

Table 2: Potential and current values obtained from potentio dynamtic polarization curve in different concentration of sulfuric acid

H_2SO_4 Concentration (N)	Potential (mV) vs. SCE at different active-passive regions						Current mA/cm^2 at different potential point			
	OCP (A)	B	C	D	E	F	B	C	D	E
0.5	−450	−370	−50	50	350	800	0.700	0.0086	0.060	0.038
1.0	−420	−370	−60	40	340	750	0.850	0.0092	0.064	0.051
2.0	−400	−350	−70	10	330	700	0.920	0.0120	0.090	0.075
5.0	−380	−350	−80	0	320	650	1.200	0.0400	0.095	0.090

OCP: Open circuit potentials, SCE: Saturated calomel electrode

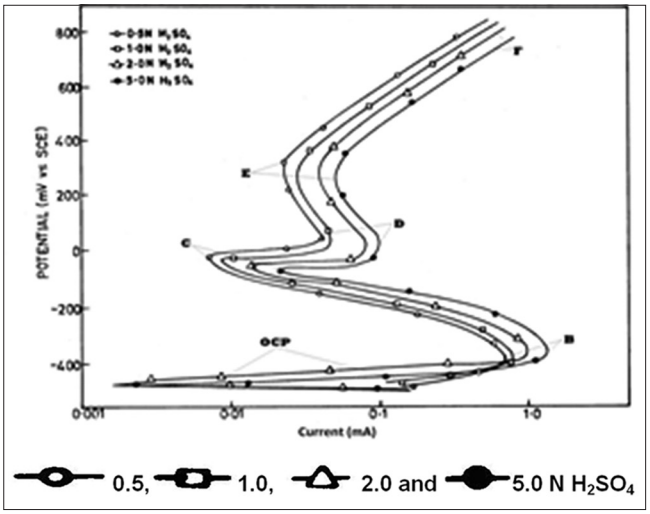

Figure 1: Potentiodynamic polarization curves for 304-stainless steel

peaks they are B, D, and C, E respectively. The transpassive potential and its current value observed at 800 mV are denoted as F.

OCP value obtained for 304-stainless steel in H_2SO_4 solution was always around −350 to −450 mV (Jallert and Quang, 1990). The increasing of acid concentration reduces the dissociation of H^+ activity, which results shifting of OCP toward an anodic direction. +70 mV variations observed between 0.5 and 5.0 N concentrations. The positive shift of OCP with increasing of acid concentration is due to enhancement of cathodic reaction rate by the reducing (proton releasing) nature of sulfuric acid.

Both the growth and thinning process of passive film formed on stainless steel results reduction in the polarization resistance during the course of increasing the acid concentrations (Ismail *et al.*, 1999). Enhancement of positive potential shift at OCP region is due to increasing of H^+ ion concentration at unit volume (increasing the specific ionic activity of proton). At potential points C to F negative shift was observed with increasing of acid concentration is due to increasing the activities of SO_4^{2-} ions. SO_4^{2-} ion activity contributes both anodic dissolution of electrode as well as film (protective layer) formation process at the surface. However, at potential point B, the observed potential shift is slightly positive direction. From this observation, it is concluded that the positive potential shift is purely influenced by H^+ ion at potential points OCP and (E_{crit}) dissolution (B) regions. The negative shift was performed by SO_4^{2-} ionic activity, which influences all passive and transpassive (F) regions.

In all potential regions in the passivation curve shows, the current values increase with increasing of acid concentration. Among the two metallic dissolutions and two passive film formed regions, the dissolution activity is maximum at point "B" and film forming process is maximum at point "C." −450 mV as OCP for stainless steel-304 in aqueous H_2SO_4 solution having pH 1 was observed (Jegdic *et al.*, 2008). In water medium, sulfuric acid dissociated to give proton and sulfate anion.

$$H_2SO_4 \rightarrow 2H^+ + SO_4^{2-} \quad (2)$$

In OCP region (−450 mV, i.e., negative potential), the proton liberated from acid influences OCP value. Increasing of acid concentration enhances the quantity of proton in the electrolyte per unit volume, which influences shifting of potential toward a positive direction. At point B the surface of electrode not having any surface layer were maximum dissolution and complete cleavage of surface layer takes place, which does not influence the usual positive side polarization. The rate of electrochemical process increases with acid concentration. Nevertheless, in the case of points C, D, E, and F the dissolved materials cover as a layer over the surface of the electrode, which acts as a barrier to polarization process cause negative shift. The activity of SO_4^{2-} ion also predominates at positive potential region. It shifts the potential toward negative direction with increasing of acid concentration.

The observed current density at dissolution potential "B" increases with acid concentration influenced by H^+ (proton) ion, which enhances the ionic activity and metal dissolution. In this region, proton attacks on the electrode surface and take up electron from metal atom present in the surface. Metal atom oxidized by the loss of electrons, which leached out from electrode structure into electrolyte. The passive layer formed at points C,

and E results minimize the current value, even though the electrochemical process enhances with increasing of acid concentration. SO_4^{2-} ion adsorbed on the surface layer formed on the electrode surface having two unit of negative charge, which induced the attractive process of positive metal ion present in the electrolyte electrostatically. In positive potential, the negative bivalent sulfate attracted on the electrode surface which attracts positive metal ion present in the electrolyte, and it combines with negative ion to form stable compound as metal oxide, hydroxide, sulfate with hydrate molecule and adsorbed on the electrode surface to make as a protective layer. The effect of SO_4^{2-} ion influences up to trans-passive region (observed from current value). The availability of sulfate ion increases with increasing acid concentration, but adsorption process takes place only up to certain critical amount of SO_4^{2-} ion up to potential region E then beyond potential point E the oxidation of surface constituents to higher valance state and oxygen evolution process predominated. The property of polarization curve and reaction mechanism performed in OCP, dissolution, passive, and transpassive potential regions discuss detailed by Yu *et al*. (2009), Wang and Northwood (2007).

The proton released from acid is adsorbed on the electrode surface during the period of absence of current impression (OCP region). The potential region at metallic dissolution (point B) proton pick-up electron from metal atom, this induces metal dissolution process. The reaction mechanism is as given.

$$nH^+ + M \rightarrow M^{n+} + nH \quad (3)$$

$$2nH \rightarrow nH_2 \uparrow \quad (4)$$

Dissolution, passivation, and depassivation on metals have been reviewed (Jayalakshmi and Muralidharan, 1994; 1996; 2003). In general dissolution of metal occurs as:

$$M + OH^- \rightleftharpoons MOH_{ads} + e \quad (5)$$

$$MOH^-ads \rightleftharpoons MOH^+_{ads} + e \quad (6)$$

$$MOH^+_{ads} \rightarrow M^{2+} + OH^- \quad (7)$$

The adsorbed intermediates cover the surface (θ MOH). The film formation may occur directly or indirectly. In indirect film formation, the film nucleation occurs in the solution. While in the direct film formation, it takes place on the surface. The dissolution-precipitation mechanism is covered by metal dissolution, pre-passive film formation, and film growth at higher potentials.

At primary passive potential region (point "C"), the dissolved metal cations present in the electrolyte are adsorbed on the electrode surface and forms primary passive protective layer, here, the film formation process is maximum. At point "D" dissolution of minor element constitute in the stainless steel is taking place, here, the dissolution process is minimum compare with potential point "B." At point "E", the metal cation present in the electrolyte made secondary passive layer having lesser protective nature than film formed at primary passive potential region. Beyond potential point "F," decomposition of passive layer results in evolution of oxygen may occur.

Qualitatively oxides of chromium, iron, and nickel were found to be more in potential point C than in potential point E. Dissolution of iron in H_2SO_4 was found to occur as (Bockris *et al*., 1961),

$$Fe + H_2O \rightleftharpoons FeOH_{ads} + H^+ + e \quad (8)$$

$$FeOH_{ads} \rightarrow FeOH^+ + e \quad (9)$$

$$FeOH^+ \rightarrow Fe^{2+} + OH^- \quad (10)$$

It is known that in 1 M sulfate and 1 M chloride solutions, iron dissolved with the formation of $Fe(OH)_2$ads (Ogura, 1980). In the presence of anodic polarization, iron dissolves through Cr_2O_3 film and reacted with H_2SO_4 to form FeOH, Fe^{2+} species.

$$FeOH + 2OH^- \rightarrow Fe(OH)_3 + 2e \quad (11)$$

Which may undergo structural changes to α-Fe_2O_3,

$$2Fe(OH)_3 \rightarrow \alpha\text{-}Fe_2O_3 + 3H_2O \quad (12)$$

And further anodic polarization favors,

$$2Fe(OH) + Fe(OH)_2 \rightarrow Fe_3O_4 + 4H^+ + 4e \quad (13)$$

In this study, chromium enrichment favored protection and increase of acid concentration enhanced iron dissolution through the film (Table 2). At moderate anodic potentials nickel, manganese dissolves to from their oxides. Sulfides incorporation in the film may also arise as the SS-304 alloy contains 0.026 weight % of sulfur. Sulfates may also be reduced the proton releasing process during polarization (chemical reaction).

In the transpassive region, oxygen evolution may occur on an oxide surface as,

$$H_2O \rightleftharpoons OH_{ads} + H^+ + e \quad (14)$$

$$OH^- + OH_{ads} \rightleftharpoons O^-_{ads} + H_2O \quad (15)$$

$$O^-_{ads} \rightleftharpoons O_{ads} + e \quad (16)$$

$$2O_{ads} \rightleftharpoons O_2\uparrow \quad (17)$$

The oxygen evolution from an oxide film involves the participation of adsorbed oxygen atom. If the desorption of oxygen atom is slow, there would accumulation of oxygen in the film taking place.

The influence of proton and formation of metal compounds are given as pictorial representation in Figure 2a and b.

Electrochemical Impedance Study

The bode plot obtained from different potential region and the corresponding parameter values are presented in Figure 3a-e and Table 3, respectively. Figure 3a shows the bode plot of steel exposed at OCP region. The charge transfer resistance values observed in k.Ohm implies the surface of the electrode having some resistive layer by adsorption of proton like particle from electrolyte. Decreasing of R_{ct} and increasing of Q_{dl} with acid conc. is due to enhancing of charge accumulation at the surface by dissolved species present in the electrolyte. The adsorbed species enhances the activity of charged species present in the surface. The steadily decreasing of resistance and increasing of capacitance (accumulation of charge) values with increasing of acid concentration at OCP region was observed from Table 3. The impedance parameters coincided with current values observed from passivation curve.

Figure 3b presents the Bode plots obtained in different concentrations of H_2SO_4 at active potential (point B) region. The curves exhibited longer horizontal and vertical regions at lower and moderate frequencies, respectively suggesting that the absence of a passive layer. The lower R_{ct} and higher Q_{dl} values which are observed at active potential region are compared with other potential region. This is due to predominant of dissolution process over film formation. Even though, the dissolution process performed at point B, the recognized value of resistance and charge accumulations are due to the presence of charged species released by dissolution of electrode surface. The ionic dissolution activity of metal present in the electrode is enhances with increasing of acid concentration.

When the log impedance plotted against log frequency (Bode plots) in the (primary passive region) at point C, the vertical region increased with H_2SO_4 concentration (Figure 3c) Solution resistance decreased with H_2SO_4 concentration implies the charged particle vacated from electrolyte to adsorb and develop the thickness of passive layer on the electrode surface. The lesser R_{ct} and higher Q_{dl}. Value observed at "C" than point "E" are due to the freshly formed porous thin protective layer.

Figure 3d presents the Bode plots obtained at point "E" in different concentrations of acid (secondary passive region). The horizontal region at higher frequency is not sharp. There is not much variation in the slopes of the vertical portions. The R_{ct} values are higher compared to those obtained in primary passivation range, and Q_{dl} values are low. Figure 3e shows the Bode plot obtained in the (transpassive region) at point "F." The R_{ct} decreased while the Q_{dl} increased. Enhancement of double layer capacitance is due to the coverage of oxygen atom on the surface of the film. At the point "F", the highest charge transfer resistance values caused by the metal ion present in the passive film having higher valance compound and the Q_{dl} values also very less.

Table 3: AC impedance parameters for 304-stainless steel in various concentration of H_2SO_4 at selective potential regions

H_2SO_4 concentrated (N)	OCP		B		C		E		F	
	R_{ct}	Q_{dl}	R_{ct}	Q_{dl}	R_{ct}	Q_{dl}	R_{ct}	Q_{dl}	R_{ct}	Q_{dl}
0.5	24.74	2.17	291	3.6	3.4	4.50	13.6	1.20	22.6	7.2
1.0	21.16	6.39	102	3.9	3.2	5.60	13.2	1.25	18.3	8.2
2.0	7.33	7.54	55	6.2	2.1	7.54	13.0	1.70	16.1	9.5
5.0	2.19	16.3	7	7.0	1.3	7.50	9.4	2.30	13.6	12.0

At OCP, C, E and F (R_{ct} = k Ω cm^{-2}, at B R_{ct} = Ω cm^{-2}, at B Q_{dl} = Ω^{-1}×10^{-3} cm^{-2}, at OCP, C and E Q_{dl} = Ω^{-1}×10^{-4} cm^{-2}, at F Q_{dl} = Ω^{-1}×10^{-5} cm^{-2}). OCP: Open circuit potentials, AC: Alternating Current

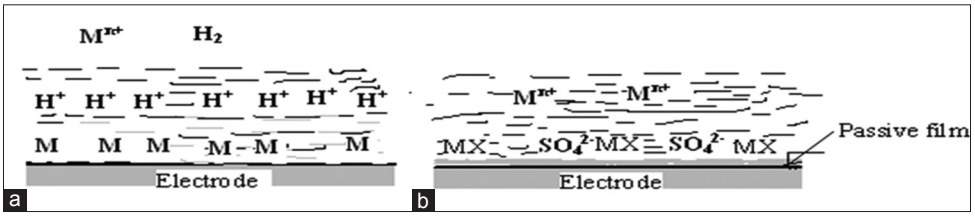

Figure 2: (a) Metal dissolution influenced by H^+ ion and (b) passivation of metal ion caused by SO_4^{2-} ion. (M: Metal atom present on the electrode structure, H^+: Proton exist in the electrolyte, M^{n+}: Dissolved metal ion present in the electrolyte, MX: Metal complex formed as a layer on the surface of electrolyte. Where, X: O, O_2, OH)

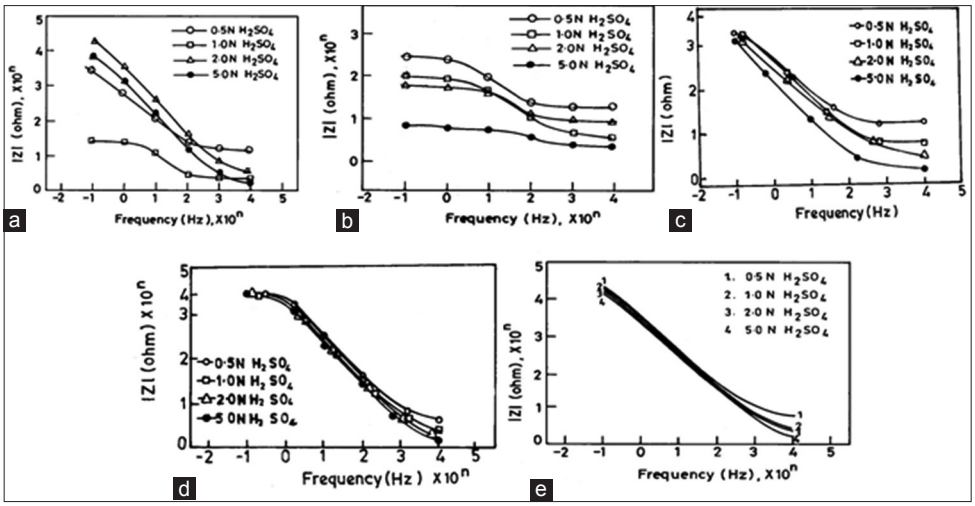

Figure 3: Bode plot taken at potential points, (a) Open circuit potentials (point A), (b) point B, (c) point C, (d) point D and (e) point F

The oxygen evolution from an oxide film involves the participation of adsorbed oxygen atom. If the desorption of oxygen atom is slow, there would be an accumulation of oxygen on the surface which changed the double layer capacitance. The same observation impedance study on the effect of acid concentration is done with study of Hermas and Morad (2008).

The observed R_{ct} values in the different passive region are in the following order:

Primary passive (C) < Secondary passive (E) < Trans-passive (F).

This may be due to formation of single passive layer at point "C," possible to the formation of the second layer at point (E) and adsorption/desorption process of oxygen molecules occur at point "F."

SEM Study

The SEM image of bare stainless steel-304 alloy is shown in Figure 4a. It is evident from the Figure 4a that the oxides of iron and chromium are formed on the grain boundary. The metal oxide shows island-like appearance. These oxides are mainly due to Fe_2O_3 and Cr_2O_3.

The scanning electron image of alloy in 0.5 N H_2SO_4 at OCP region is shown in Figure 4b. The metal oxide formed on the surface is covered by metal hydrate and metal hydroxides. These hydroxides are of smooth and uniform structure, and they are found to cover the surface completely.

The surface appearance at potential region of point C is represented through Figure 4c. The iron, chromium and nickel hydroxides, and sulfate constituents were adsorbed on the surface are not uniformly covered but adsorbed scatterly on the surface.

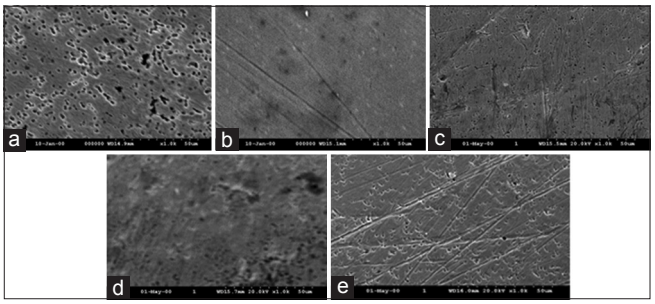

Figure 4: The scanning electron microscopic image of: (a) Bare304-stainless steel surface (without immersed), (b) immersed in 0.5 N H_2SO_4 at open circuit potentials, (c) potential point C, (d) potential point E and (e) potential point F

At potential point E, thicker layer is formed on the surface as is shown in Figure 4d. Metal oxide and hydroxides are agglomerated throughout the surface along with sulfate. At potential region F, the passive layer is dissolved, and grain boundaries present in the surface appear clearly. The higher valence metal oxides and oxygen spread over the surface, but not uniformly. The surface morphology of 304-stainless steel at trans-passive region is shown in Figure 3e.

X-ray Photoelectron Microscopic Investigation

Table 4 summarizes species identified on the film obtained in the potential points E and F. XPS studies revealed an enrichment of chromium in passive film at the primary range in 0.5 N H_2SO_4 while increase of acid concentration favored iron enrichment in the secondary passive range. Oxides enrichment was higher in dilute acid. Film

formation required less coulombs of electricity in dilute acid. Higher acid concentration favored dissolution.

In this study, the observed peaks at 530.1 eV, 531.5 eV, and 533.0 eV suggest the presence of oxygen as O^{2-} and OH^- ions. Water is bound inside the film. Desorption and dehydration of water molecules favor the film growth. The film may contain M-H_2O bonds as H_2O-M-H_2O, HO-MOH, or O-M-O. Depending on the anodic potential, film grows. The film on stainless steel was found earlier to be polycrystalline (Clayton *et al.*, 1983). Sulfate ions adsorb on the surface and favor to form H_2O-SO_4^{2-} bonds. On Fe-Cr (13%) alloy, the passive film was found to contain hydrated chromium hydroxide on the chromium rich inner layer, OH^- ions, and adsorbed water molecules on this inner layer. In H_2SO_4/Na_2SO_4 solutions, the film contained iron oxide, hydroxide, and chromium (Asami *et al.*, 1978; Castle and Clayton, 1977). In this study in the primary passivation range Cr_2O_3, CrOOH species were identified.

The observed peaks at 706.82 eV and 723.98 eV confirm the presence of $Fe(OH)_3$. The presence of α-Fe_2O_3 was confirmed by the peaks at 724.30 eV and 725.27 eV. α-FeOOH presence was indicated by the peaks at 724.97 eV and 711.44 eV.

It was shown that a surface of stainless steel exposed to deaerated 1 M H_2SO_4 + 0.5 M HCl solution (Hermas, 1999) on anodic polarization, the surface was found to contain surface Cr-rich oxide film responsible for maintaining passivity of stainless steel. This enrichment of Cr in the passive film of Fe–Cr alloys and stainless steel was due to both the lower mobility of Cr in the film and the preferential dissolution of iron into the electrolyte. The Cr-rich film was suggested to consist of a hydrated form of CrOOH (Asami *et al.*, 1976; Sugimoto and Sawada, 1977) while Olefjord claimed that Cr_2O_3 was the main passivating compound (Olefjord and Brox, 1983).

In the initial passivating process, it was suggested that Cr directly reacts with water to form Cr_2O_3, followed by the formation of $Cr(OH)_3$ at the oxide-solution interface. The iron oxyhydroxide or iron hydroxide appears to be formed with $Cr(OH)_3$, resulting in the formation of a duplex hydroxide layer (Schmuki *et al.*, 1993). On the chromium oxide, the dissolved iron formed oxide such as $\alpha.Fe_2O_3$ and Fe_3O_4. Further polarization enriches the chromium content in the film. The nature of the semiconducting passive film changes on polarization (Ogura, 1980). Changes in double layer capacitances with acid concentration and anodic potentials suggest that the transition occurs from n-type to p-type conductivity (Yang *et al.*, 1999). Photoelectrochemical studies in 0.05M H_2SO_4 revealed that the protective property of the film depends on chromium content in the alloy (Duret-Thual and Barrau, 1983; Okamoto, 1973; Natarajan *et al.*, 2009).

Table 4: Summary of the compounds likely to be present in the passive film – XPS study

At potential point C	At potential point E
CrOOH, Cr_2O_3, CrO_3, γ-Fe_2O_3, γ-FeOOH, Mn_2O_3, Mn_3O_4, MnS, $Ni(OH)_2$, Ni_2O_3, $NiOS^-$, SO_4^{2-}	Cr_2O_3, $Cr(OH)_3$, CrO_3, $Fe(OH)_3$, α-Fe_2O_3, γ-FeOOH, Fe_3O_4, α-FeOOH, Mn_2O_3, Mn_3O_4, MnS, MnO_2, NiO, $Ni(OH)_2$, S^{2-}, SO_4^{2-}

XPS: X-ray photoelectron spectroscopy

CONCLUSION

The activity of H^+ predominates at OCP and active (potential point B) region, which shifts the potential toward positive direction. SO_4^{2-} ion influences in anodic dissolution and film formation reaction. The direct relationship observed on current consumption with acid concentration throughout entire potential region is due to increasing the specific activity of H^+ ion. XPS studies revealed the existence of CrOOH, Cr_2O_3, γFe_2O_3, γFeOOH, Mn_2O_3, Mn_3O_4, MnS, $Ni(OH)_2$, Ni_2O_3, NiO, and sulfide ion at the oxide - electrolyte interface. The passive film was found to contain chromium oxide inner layer and the dissolution of iron caused the formation of oxides of iron namely αFe_2O_3 and γFeOOH. Higher oxides of manganese and nickel are also observed due to the dissolution of the film. Sulfates are reduced to sulfur chemically by the released protons from anodic polarization.

REFERENCES

Abdallah M. Corrosion behavior of 304 stainless steel in sulphuric acid solutions and its inhibition by some substituted pyrazolones. Mater Chem Physics 2003;82:786-92.

Asami K, Hashimoto K, Shimodaira S. An ESCA study of the Fe^{2+}/Fe^{3+} ratio in passive films on iron-chromium alloys. Corros Sci 1976;1:387-91.

Asami K, Hashimoto K, Shimodaira S. An XPS study of the passivity of a series of iron-chromium alloys in sulphuric acid. Corros Sci 1978;18:151-60.

ASM. Hand Book. Vol. 13b. Park, OH, USA: Corrosion Material ASM International; 2005. p. 28.

Bockris JO, Drazic D, Despic AR. The electrode kinetics of the deposition and dissolution of iron. Electrochim Acta 1961;4:325-61.

Castle JE, Clayton CR. The use of in the x-ray photo-electron spectroscopy analyses of passive layers on stainless steel. Corros Sci 1977;17:7-26.

Clayton CR, Doss K, Warren JB. In: Froment M, editor. Passivity of Metals and Semiconductors. Bombannes: Elsevier; 1983. p. 585-90.

Duret-Thual C, Barrau F. Modification of passive films. In: Marcus P, Baroux B, Keddam M, editors. European Federation of Corrosion. Vol. 12. London: The Institute Mater; 1993. p. 176-88.

Hermas AA, Morad MS. A comparative study on the corrosion behavior of 304 austenitic stainless steel in sulfamic and sulfuric acid solutions. Corros Sci 2008;50:2710-7.

Hermas AA. Polarisation of low phosphorus AISI 304 Stainless steel in sulphuric acid containing arsenites. Br Corros J 1999;34:132-8.

Ismail KM, Jayaraman A, Wood TK, Earthman JC. The influence of bacteria on the passive film stability of 304 stainless steel. Electrochim Acta 1999;44:4685-92.

Jallert N, Quang KV. Passivation of Ni-Cr-Mo alloys in chloride solution a new kinetics. Corros Sci 1990;31:539-44.

Jamialahmadi M, Muller-Steinhagen H. Heat exchanger fouling and cleaning in the Dihydrate process for the production of Phosphoric acid. Trans I Chem E Part A Chem Eng Res Des 2007;85:245-55.

Jayalakshmi M, Muralidharan VS. Empirical and deterministic model of pitting corrosion - On overview. Corros Rev 1996;14:375-402.

Jayalakshmi M, Muralidharan VS. Role of anions in the dissolution passivation and pitting of metals - A review. Corros Rev 2003;21:327-47.

Jayalakshmi M, Muralidharan VS. Sulphur induced depassivation of transition metals in alkali solutions. Corros Rev 1994;12:359-75.

Louie DK. Hand Book of Sulfuric Acid Manufacturing. 2nd ed. Ch. 26. New York: DKL. Engineering Inc.; 2008. p. 4-17.

Jegdic B, Drazic DM, Popic JP. Open circuit potentials of metallic chromium and austenitic 304 stainless steel in aqueous sulphuric acid solution and the influence of chloride ions on them. Corros Sci 2008;50:1235-44.

Kish JR, Ives MB, Rodda JR. Anodic behavior of stainless steel S43000 in concentrated solutions of sulphuric acid. Corros Sci 2003;45:1571-94.

Kumagai M, Myung ST, Kuwata S, Asaishi R, Yashiro H. Corrosion behavior of austenitic stainless steels as a function of pH for use as bipolar plates in polymer electrolyte membrane fuel cells. Electrochim Acta 2008;53:4205-12.

Natarajan R, Palaniswamy N, Natesan M, Muralidharan VS. XPS analysis of passive film on stainless steel. Open Corros J 2009;2:30-40.

Ogura KA. Dissolution-precipitation model for metal passivation. Electrochem Acta 1980;25:335-9.

Okamoto G. Passive film of 18.8 stainless steel structure and its function. Corros Sci 1973;13:471-89.

Olefjord I, Brox B. Quantitative ESCA analysis of the passive state of an Fe-Cr-alloy and Fe-Cr-Mo alloy, ibid (26). Passivity of Metals and Semiconductors. Amsterdam: Elsevier; 1983. p. 561.

Raja KS, Jones DA. Effects of dissolved oxygen on passive behavior of stainless alloys. Corros Sci 2006;48:1623-38.

Ren YJ, Zeng CL. Corrosion protection of 304 stainless steel bipolar plates using TiC films produced by high-energy micro-arc alloying process. J Power Sources 2007;171:778-82.

Riggs Jr OL, Locke CE. Anodic protection, Theory and Practice in the Prevention of Corrosion. New York: Plenum Press; 1981. p. 25.

Schmuki P, Bohni H, Mansfeld F. A photo electrochemical investigation of passive films formed by alternating voltage passivation. J Electrochem Soc 1993;140:L119.

Sugimoto K, Sawada Y. The role of molybdenum additions to austenitic stainless steels in the inhibition of pitting in acid chloride solutions. Corros Sci 1977;17:425-45.

Wang Y, Northwood DO. An investigation into TiN-coated 316L stainless steel as a bipolar plate material for PEM fuel cells. J Power Sources 2007;165:293-8.

Yang MZ, Luo JL, Patchet BM. Correlation of hydrogen-facilitated pitting of AISI 304 stainless steel to semi conductivity of passive films. Thin Solid Films 1999;354:142-7.

Yu H, Yang L, Zhu L, Jian X, Wang Z, Jiang L. Anticorrosion properties of Ta-coated 316L stainless steel as bipolar plate material in proton exchange membrane fuel cells. J Power Sources 2009;191:495-500.